Virologica Sinica 39 (2024) 123–133

Contents lists available at ScienceDirect

Virologica Sinica

journal homepage: www.keaipublishing.com/en/journals/virologica-sinica
www.virosin.org

Research Article

Drug repurposing screen identifies vidofludimus calcium and pyrazofurin as novel chemical entities for the development of hepatitis E interventions

Hongbo Guo [a,*,1], Dan Liu [a,1], Kuan Liu [b,c,1], Yao Hou [a], Chunyang Li [a], Qiudi Li [a], Xiaohui Ding [a], Monique M.A. Verstegen [c], Jikai Zhang [a], Lingli Wang [a], Yibo Ding [a], Renxian Tang [a], Xiucheng Pan [d], Kuiyang Zheng [a], Luc J.W. van der Laan [c], Qiuwei Pan [b,*], Wenshi Wang [a,*]

[a] Department of Pathogen Biology and Immunology, Jiangsu Key Laboratory of Immunity and Metabolism, Jiangsu International Laboratory of Immunity and Metabolism, Xuzhou Medical University, Xuzhou, 221004, China
[b] Department of Gastroenterology and Hepatology, Erasmus MC-University Medical Center, Rotterdam, NL-3015 CN, the Netherlands
[c] Department of Surgery, Erasmus MC Transplant Institute, University Medical Center, Rotterdam, 3015CE, NL-3015 CN, the Netherlands
[d] Department of Infectious Diseases, The Affiliated Hospital of Xuzhou Medical University, Xuzhou, 221002, China

ARTICLE INFO

Keywords:
Hepatitis E virus (HEV)
Drug repurposing
Vidofludimus calcium
Pyrazofurin
Pyrimidine biosynthesis

ABSTRACT

Hepatitis E virus (HEV) infection can cause severe complications and high mortality, particularly in pregnant women, organ transplant recipients, individuals with pre-existing liver disease and immunosuppressed patients. However, there are still unmet needs for treating chronic HEV infections. Herein, we screened a best-in-class drug repurposing library consisting of 262 drugs/compounds. Upon screening, we identified vidofludimus calcium and pyrazofurin as novel anti-HEV entities. Vidofludimus calcium is the next-generation dihydroorotate dehydrogenase (DHODH) inhibitor in the phase 3 pipeline to treat autoimmune diseases or SARS-CoV-2 infection. Pyrazofurin selectively targets uridine monophosphate synthetase (UMPS). Their anti-HEV effects were further investigated in a range of cell culture models and human liver organoids models with wild type HEV strains and ribavirin treatment failure-associated HEV strains. Encouragingly, both drugs exhibited a sizeable therapeutic window against HEV. For instance, the IC_{50} value of vidofludimus calcium is 4.6–7.6-fold lower than the current therapeutic doses in patients. Mechanistically, their anti-HEV mode of action depends on the blockage of pyrimidine synthesis. Notably, two drugs robustly inhibited ribavirin treatment failure-associated HEV mutants (Y1320H, G1634R). Their combination with IFN-α resulted in synergistic antiviral activity. In conclusion, we identified vidofludimus calcium and pyrazofurin as potent candidates for the treatment of HEV infections. Based on their antiviral potency, and also the favorable safety profile identified in clinical studies, our study supports the initiation of clinical studies to repurpose these drugs for treating chronic hepatitis E.

1. Introduction

Hepatitis E virus (HEV) is the most common cause of viral hepatitis worldwide. It is estimated that 939 million individuals, corresponding to 1 in 8 people, having ever experienced HEV infection. 15–110 million individuals have recent or ongoing HEV infection (Li et al., 2020). Notably, these estimates are based on studies that employ assays now known to have inferior sensitivity. As such, the true global burden of hepatitis E related disease is likely underestimated (Webb and Dalton, 2019). In resource limited settings (e.g., among refugees and internally displaced groups), HEV continuously causes large outbreaks and presents significant humanitarian emergencies (Desai et al., 2022). In developed regions, HEV commonly causes zoonotic food-borne infections (Velavan et al., 2021). An acute infection can be aggravated in pregnant women and patients with pre-existing liver disease, resulting in severe complications and high mortality (Webb and Dalton, 2019). Chronic infection can be developed in immunosuppressed patients, in particular organ transplant recipients.

Currently, there are no approved drugs specifically designed for the treatment of HEV infections. Chronic hepatitis E patients are occasionally treated with broad-spectrum antivirals, pegylated interferon-alpha (PegIFN-α) and ribavirin. However, the use of PegIFN-α is limited due

* Corresponding authors.
E-mail addresses: Hongbo.guo@xzhmu.edu.cn (H. Guo), q.pan@erasmusmc.nl (Q. Pan), wenshi.wang@xzhmu.edu.cn (W. Wang).
[1] Hongbo Guo, Dan Liu and Kuan Liu contributed equally to this work.

https://doi.org/10.1016/j.virs.2023.11.006
Received 5 August 2023; Accepted 16 November 2023
Available online 19 November 2023

to its immunostimulatory properties, which can induce acute rejection. Therefore, PegIFN-α cannot be used in transplant patients, particularly in heart-, lung-, pancreas- or kidney-transplant patients (Kamar et al., 2022). Ribavirin is relatively effective in treating chronic HEV infection. However, a proportion of patients either does not respond to treatment or remain viremic despite long-term ribavirin treatment (Kamar et al., 2014). Moreover, ribavirin-associated mutations in HEV RNA polymerase may increase the replication capacity of HEV, thereby complicating the disease outcomes (Debing et al., 2014, 2016; Wang et al., 2023). Lastly, both PegIFN-α and ribavirin are contraindicated for use in pregnant women (Kinast et al., 2019). These contemporary challenges highlight the unmet needs in drug development for curing hepatitis E.

The process of developing novel drugs is typically laborious, costly, and failure-prone. Thus, it is unappealing to do so for HEV. In contrast, repurposing existing drugs for new indications represents a time-saving and cost-efficient approach, resulting in higher success rates (Roessler et al., 2021). The current first choice of anti-HEV treatment, ribavirin, is a successful example of a repurposed drug originally developed for treating respiratory syncytial virus in infants (Mcbride, 1985). Following this strategy, several periclinal antiviral candidates, including 2′-C-methylcytidine, NITD008 and GPC-N114 have been identified as anti-HEV candidates in experimental models (Qu et al., 2017; Netzler et al., 2019). However, no ongoing clinical trials have been registered, and some developmental efforts were discontinued due to adverse toxic effects (Kinast et al., 2019).

Given the public availability of drugs or drug candidates with elucidated pharmacokinetics, pharmacodynamics, and safety information, we screened an antiviral agent library consisting of 262 drugs/compounds. Most of the candidates have passed safety assessments, entered the clinical development pipeline or been approved by FDA. Through repurposing screening, we identified vidofludimus calcium and pyrazofurin as potent antivirals against HEV. Vidofludimus calcium is the next-generation dihydroorotate dehydrogenase (DHODH) inhibitor (Muehler et al., 2020b). Pyrazofurin selectively targets uridine monophosphate synthetase (UMPS) (Wang et al., 2021). Both targets are the rate-limiting enzymes of *de novo* pyrimidine biosynthesis. The potent antiviral efficacy of these two drugs was firmly confirmed in both HEV replicon and infectious models supported by human primary liver organoids derived from four donors (two male and two female). Mechanistically, their anti-HEV mode of action was achieved by the blockage of pyrimidine synthesis, a crucial process for viral replication. Significantly, these two drugs also robustly inhibited ribavirin treatment failure-associated HEV mutants (Y1320H, G1634R). Combination with IFN-α resulted in synergistic antiviral activity. These two drugs have advanced or completed phase 2 or 3 clinical trials in the drug development pipeline. This study indicates that two drugs we identified bear huge potential for being repurposed as novel interventions for chronic hepatitis E.

2. Materials and methods

2.1. Reagents and antibodies

A library of 262 board-spectrum chemical compounds was kept in 96-well plate format with a concentration of 10 mmol/L. The list of compounds is provided in Supplementary Table S1. Vidofludimus (Selleck, USA, S7262) was dissolved in dimethyl sulfoxide (DMSO) with a stock concentration of 10 mmol/L. Pyrazofurin (Sigma-Aldrich, USA, SML1502) was dissolved in H_2O with a stock concentration of 10 mmol/L. Uridine (Merck, USA, U3750) was dissolved in H_2O with a stock concentration of 10 mmol/L. Ribavirin (Merck, USA, R9644) was dissolved in DMSO with a stock concentration of 10 mmol/L. Human interferon Alpha 2A (PBL assay science, USA, 11100-1) was dissolved in phosphate buffered saline (PBS) supplemented with 0.1% bovine serum albumin (BSA). HEV ORF2 polyclonal antibody was kept in our laboratory. Anti-rabbit, anti-mouse peroxidase-conjugated and anti-rabbit 594-conjugated secondary antibodies were purchased from Jackson ImmunoResearch (USA). GAPDH antibody (60004-1-lg) was obtained from Proteintech (China).

2.2. Cell culture

Human hepatoma HuH7 cell line, and human embryonic kidney cell line (HEK293T) were cultured in Dulbecco's modified Eagle's medium (DMEM) (SenBeiJia Biological Technology, China) supplemented with 10% heat-inactivated fetal bovine serum (FBS) (Sigma-Aldrich, USA, F2442) in a humidified 5% CO_2 incubator at 37 °C.

2.3. Human liver-derived organoids

The isolation and culture of organoids were conducted using liver tissues obtained during liver transplantation at the Erasmus Medical Center Rotterdam. The utilization of liver tissues for research was approved by the Medical Ethical Council of the Erasmus MC, with informed consent obtained from donors (MEC-2014-060). Organoids were cultured in organoid expansion medium (EM) composed of advanced DMEM/F12 (Invitrogen, USA) supplemented with 1% penicillin/streptomycin (Life Technologies, USA), 1 mol/L Hepes (Life Technologies, USA), 200 mmol/L ultraglutamine (Life Technologies, USA), 1% (v/v) of N_2 (Gibco), 2% (v/v) of B27 (Gibco, USA), 1 mmol/L N-acetylcysteine (Sigma-Aldrich, USA), 10 mmol/L nicotinamide (Sigma-Aldrich, USA), 5 μmol/L A83.01 (Tocris, UK), 10 μmol/L forskolin (Tocris, UK), 10 nmol/L gastrin (Sigma-Aldrich, USA), epidermal growth factor (EGF) (50 ng/mL; PeproTech, USA), 10% (v/v) of R-spondin-1 (conditioned medium), fibroblast growth factor 10 (FGF10) (100 ng/mL; PeproTech, USA), hepatocyte growth factor (HGF) (25 ng/mL; PeproTech, USA), and 10 μmol/L Y27632 (Sigma-Aldrich, USA).

2.4. Viruses and HEV models

Plasmid constructs containing the full-length HEV genome (Kernow-C1 p6 clone; GenBank Accession Number JQ679013), variants harboring RNA-dependent RNA polymerase mutants (M1: Y1320H, M2: G1634R), a double mutant (M1+2: G1634R/Y1320H), a replication defective mutant GAD, and subgenomic HEV replicon with a Gaussia luciferase reporter gene were transcribed into RNA *in vitro* by using mMessage mMachine T7 RNA kits (Invitrogen) (Shukla et al., 2012).

HEV genomic RNA was delivered into HuH7 and HEK293T cells by electroporation as previously described (Qu et al., 2017; Li et al., 2022). HuH7 and HEK293T cells support the full life cycle of HEV. After electroporation, HEV RNA replicates stably within cells for six to eight generations. For HEV-related *Gaussia* luciferase analysis, the activity of secreted luciferase in the culture supernatant was measured by the *Gaussia* Luciferase Reporter Gene Assay Kit (Beyotime, China, RG021 M).

For organoids based HEV model, HEV genomic RNA was introduced into human-derived liver organoids by electroporation as previously described (Li et al., 2022). In short, organoids were collected in cold Advance DMEM/F12 medium when becoming confluent enough. Next, organoids were resuspended in Opti-MEM followed by pipetting up and down by 15 times. 200 μl organoids suspension and 6 μg HEV RNA were mixed thoroughly and added into 4-mm electroporation curve (Cellprojects, UK), and electroporation was performed according to the following configured program: voltage, 700 V; pulse length, 4 ms; pulse interval, 0 s; number of pulses, 1. After three times rinsing with Opti-MEM to eliminate residual RNA, the organoids were then embedded in matrigel and cultured at 37 °C with 5% CO_2 in EM. After electroporation, HEV genomic RNA initiates its replication and produces progeny virions. The three-dimensional cultured organoids support the full life cycle of HEV infection, which serves as a state-of-art model for development of antivirals.

2.5. Cell viability assay

WST-1 reagent from cell proliferation and viability detection kit (KeyGen Biotech, KGA316, China) was added to the cells in 96-well plate. Cells were maintained at 37 °C with 5% CO_2 for 3 h. The absorbance of each well was read on the microplate absorbance readers (BIO-RAD, USA) at wavelength of 450 nm.

2.6. AlamarBlue assay

The culture supernatant of the organoids was removed. The organoids were incubated with alamarBlue (Invitrogen, USA, DAL1100; diluted 1:20 in organoid expansion medium) for a duration of 2 h at 37 °C. Following this, the entire medium was collected to evaluate the metabolic activity of the organoids. Absorbance measurements were performed using a fluorescence plate reader (CytoFluor Series 4000, PerSeptive Biosystems, USA) with excitation at 530/25 nm and emission at 590/35 nm.

2.7. Quantification of viral replication

Total RNA was extracted using TRIzol Reagent (Absin, China, abs9331) according to the manufacturer's protocol. After reverse-transcribed into cDNA, HEV RNA was quantitated by SYBR-Green-based RT-qPCR (2X SYBR Green qPCR Master Mix, APExBIO, USA). GAPDH was used as a housekeeping gene to normalize gene expression using the $2^{-\Delta\Delta Ct}$ ($\Delta\Delta Ct = \Delta CTsample\text{-}\Delta CTcontrol$) formula. HEV primers: HEV-F, TTGCCTCCGAGTTAGTCATC; HEV-R, TGCAAAGCATTACCAGACCG. GAPDH primers: GAPDH-F, GTCTCCTCTGACTTCAACAGCG; GAPDH-R, ACCACCCTGTTGCTGTAGCCAA.

2.8. Immunofluorescence assay

Cells were fixed in 4% paraformaldehyde solution at room temperature (RT) for 30 min, rinsed twice times with PBS for 5 min each time, and permeabilized with PBS containing 0.3% Triton X-100 for 15 min. Then, cells were rinsed twice with PBS for 5 min, followed by incubation with blocking solution (5% skim milk in PBS) at RT for 1 h. Next, cells were incubated with anti-ORF2 polyclonal antibody (dilution:1 : 3000) at 4 °C overnight, followed by 1 h incubation with secondary antibody (AlexaFluor 594, dilution:1:10000). Nuclei were stained with Hoechst Stains (dilution: 1 : 500) (Invitrogen, USA).

Organoids were fixed in 4% paraformaldehyde solution for 10 min. The organoids were then rinsed three times with PBS for 5 min each time, followed by permeabilizing with PBS containing 0.2% (v/v) Triton X-100 for 5 min. Then, the organoids were rinsed twice with PBS for 5 min, followed by incubation with blocking solution (2% bovine serum albumin in PBS) at room temperature for 1 h. Next, the organoids were incubated in a humidity chamber with primary antibody diluted in blocking solution at 4 °C overnight. Primary antibodies used in this study are as follows: Anti–HEV ORF2 antibody (1:250, mouse monoclonal antibody (mAb); Millipore, USA, MAB8002), anti-EpCAM antibody (1:1000, rabbit mAb; Abcam, UK). The organoids were washed three times for 5 min each in PBS before 1 h incubation with anti-mouse immunoglobulin G (IgG) (H + L, Alexa Fluor 594, dilution: 1:1000), or the anti-rabbit IgG (H + L, Alexa Fluor 647, dilution: 1:1000). Finally, nuclei were stained with 4′,6-diamidino-2-phenylindole (Invitrogen, USA).

2.9. Western blot assay

Proteins in cell lysates were harvested using 3× denaturing loading buffer and heated at 95 °C for 5 min, whereas proteins in the cell supernatant were harvested and mixed with non-denaturing loading buffer without boiling. Protein samples were loaded onto a 10% sodium dodecyl sulfate polyacrylamide gel (SDS-PAGE), separated at 120 V for 90 min, and transferred onto a polyvinylidene difluoride (PVDF) membrane (pore size: 0.45 mm; BIO-RAD) for 100 min with an electric current of 250 mA. Subsequently, the membrane was blocked with blocking buffer (5% skim milk in PBS). Membrane was followed by incubation with primary antibodies rabbit anti-ORF2 (1:4000) or anti-GAPDH (1:5000) overnight at 4 °C. The membrane was washed 3 times, and followed by incubation for 1 h with anti-rabbit or anti-mouse HRP-conjugated secondary antibodies (1:10000, Jackson, USA) at room temperature. After washing 3 times, protein bands were detected with BIO-RAD Imaging System.

2.10. Statistical analysis

All results were presented as mean ± standard errors of the means (SEM). The significance of differences was assessed by a one-way analysis of variance (ANOVA), with differences among groups assessed by GraphPad Prism. $^{*}P < 0.05$, $^{**}P < 0.01$, $^{***}P < 0.001$ was considered to indicate statistical significance. Synergistic score of drug combinations were analyzed by SynergyFinder 3.0 (https://synergyfinder.fimm.fi/) (Ianevski et al., 2022).

3. Results

3.1. Drug repurposing screen identifies vidofludimus calcium and pyrazofurin as novel anti-HEV entities

We screened a best-in-class drug repurposing library consisting of 262 drugs/compounds. The tropism of HEV is not restricted to the liver, and virus replication was demonstrated in multiple organs (Kamar et al., 2015, 2016; Pischke et al., 2017). The extra-hepatic manifestations of HEV infection, e.g., in the kidney and the nervous system have also been reported (Del Bello et al., 2015; Guinault et al., 2016; Karki et al., 2016). Therefore, both hepatic (HuH7) and non-hepatic (HEK293T) cell lines were used in our screening. This ensured that the drug candidates identified could inhibit HEV replication in multiple cells. Both HEV replicon model and HEV full-length genome efficiently replicate in HEK293T and HuH7 cell (Supplementary Fig. S1). The initial screening was performed in both HEK293T and HuH7 cell-based genotype 3 HEV replicon models in which the 5' portion of HEV ORF2 was replaced with the in-frame secreted form of *Gaussia* luciferase. Two models were treated with each compound at a concentration of 10 μmol/L or DMSO vehicle control. HEV replication-related luciferase activity and cell viability were determined at 72 h post-treatment (Fig. 1A). Ribavirin was included in the screening as a positive control. Hits were selected based on the demonstration of >50% reduction in luciferase values and <20% cytotoxicity. Herein, we identified 40 (in HEK293T) and 49 (in HuH7) compounds capable of inhibiting HEV replication. Notably, most hits are cell-line specific, likely due to different host cell-specific sensitivities to modulators. Eighteen candidates reduced HEV replication in both cell models (Fig. 1B). Among these hits, vidofludimus calcium and pyrazofurin possess desirable anti-HEV activity in both cell models, and thus were subjected to further detailed study (Fig. 1C and D).

Next, we evaluated the antiviral effects of these two drugs in both HuH7 cell-based genotype 3 HEV replicon models and HEV infectious models. These two drugs showed potent antiviral activity against HEV (Fig. 2A–E). For instance, vidofludimus calcium (5 μmol/L) and pyrazofurin (1 μmol/L) inhibited HEV replication to 40%, which is comparable to the antiviral effect of ribavirin (5 μmol/L). Consistently, immunofluorescent staining of ORF2 protein showed dramatic reduction of the number of infected cells post-treatment (Fig. 2F and G). The levels of intracellular and extracellular ORF2 protein were also significantly decreased (Fig. 2H and I). Importantly, we observed large therapeutic windows between the half-maximum cytotoxic concentration (CC_{50}) and half-maximal inhibitory concentration (IC_{50}) values. Specifically, the selectivity index (SI) values of vidofludimus calcium and pyrazofurin were 63 and 2444, respectively (Table 1).

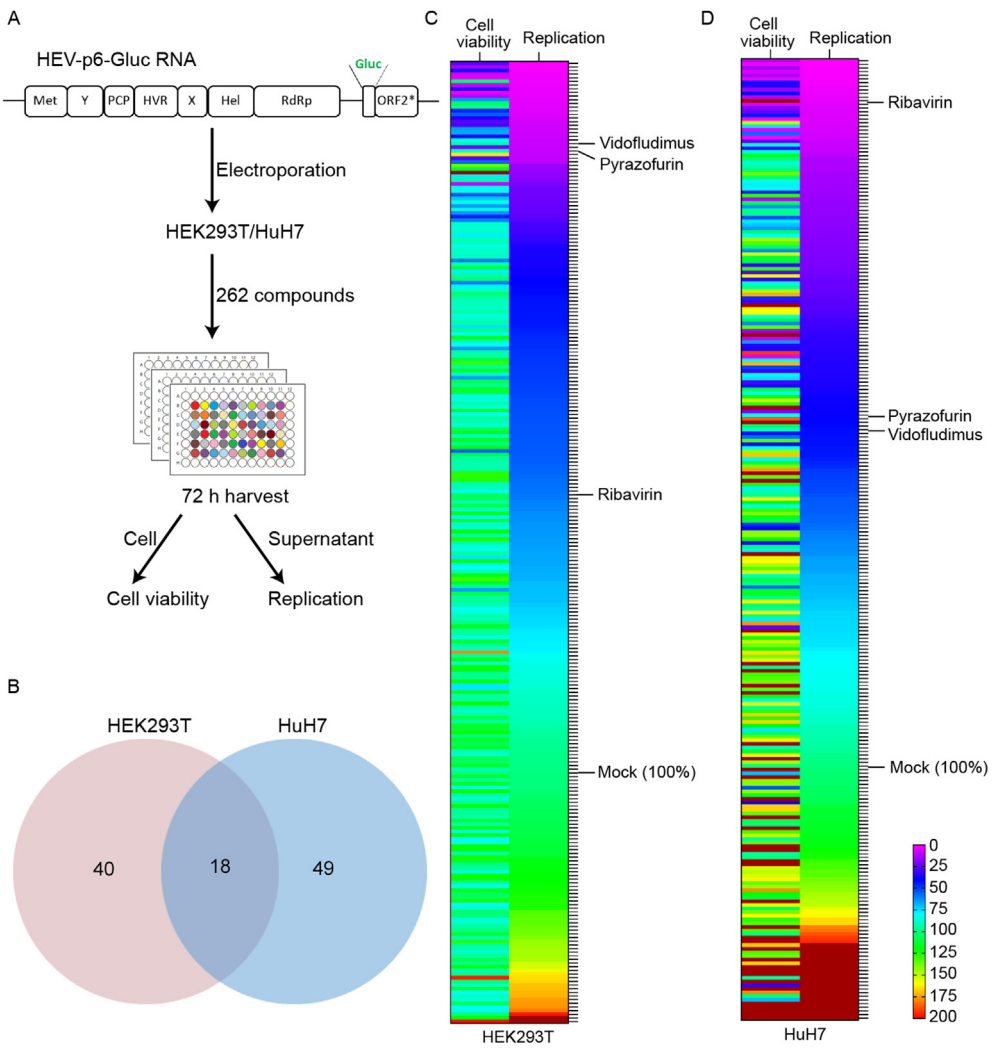

Fig. 1. Drug repurposing screen identified vidofludimus calcium and pyrazofurin as potent inhibitors against HEV replication. **A** Schematic illustration of the screening flow chart. HEK293T or HuH7 cell-based HEV replicon models were treated with 262 compounds at 10 μmol/L. HEV replication-related luciferase activity and cell viability were determined 72 h post-treatment. **B** Venn diagram showed that 18 compounds inhibited HEV replication in both cell models (<50%) without significantly affecting cell viability (>80%). **C–D** Heatmap showed the effect of compounds on cell viability and HEV replication of HEK293T (**C**) and HuH7 (**D**) cell lines (n = 6). Mock, untreated control. Data were normalized to the Mock control (set as 100%).

3.2. Vidofludimus calcium and pyrazofurin exert potent anti-HEV effect through the depletion of pyrimidine nucleotide pool

In the *de novo* biosynthesis pathway of pyrimidines, DHODH and UMPS are sequentially the fourth and fifth, as well as the rate-limiting enzymes. DHODH is located in the inner membrane of mitochondria, where it converts dihydroorotate to orotate. Then, the multifunctional UMPS uses orotate to produce UMP, one of the essential precursors for the synthesis of all other pyrimidine nucleotides (Fig. 3A). We and others have previously reported that suppression of pyrimidine biosynthesis robustly inhibits a range of different viruses (Wang et al., 2016; Chen et al., 2019; Xiong et al., 2020). Vidofludimus calcium is the newly developed next-generation DHODH inhibitor, and pyrazofurin selectively targets UMPS (Muehler et al., 2020b). Exogenous uridine was supplemented to investigate whether these two drugs exerted their anti-HEV effect via the modulation of pyrimidine biosynthesis. Notably, RT-qPCR results indicated that uridine supplementation dose-dependently abolished the anti-HEV effect of two drugs (Fig. 3B). Indirect fluorescence microscopy and western blot analysis further confirmed that exogenous uridine could largely suppress the drug-related anti-HEV effect, especially at the concentration of 500 μmol/L (Fig. 3C–D and Supplementary Fig. S2). In sum, vidofludimus calcium and pyrazofurin exert their anti-HEV effect by suppressing the pyrimidine nucleotide pool.

3.3. Vidofludimus calcium and pyrazofurin robustly inhibit HEV replication in human primary liver organoids

Vidofludimus calcium and pyrazofurin are host-targeting antivirals. Hence, profile the drug efficacy in a more physiologically relevant human model is essential. In this respect, HEV-liver organoids models have been successfully established (Li et al., 2022). This state-of-art system retains human genetic information and physiological function, and supports the full life cycle of HEV infection. Thus, we further validated the potency of these two drugs in human primary liver organoids based HEV models. To evaluate drug responses among different individuals, which will facilitate the development of personalized treatment, organoids from four different donors were employed (donor 1: male, donor 2: female, donor 3: male, donor 4: female) (Supplementary Fig. S3). Vidofludimus calcium showed comparable antiviral efficacy in donor 1 (IC_{50}: 1.08 μmol/L) and donor 2 (IC_{50}: 1.20 μmol/L), and much more potent in donor 3 (IC_{50}: 0.01 μmol/L) and donor 4 (IC_{50}: 0.01 μmol/L) (Fig. 4A, and Supplementary Fig. S4A–D). Pyrazofurin is more sensitive to donor

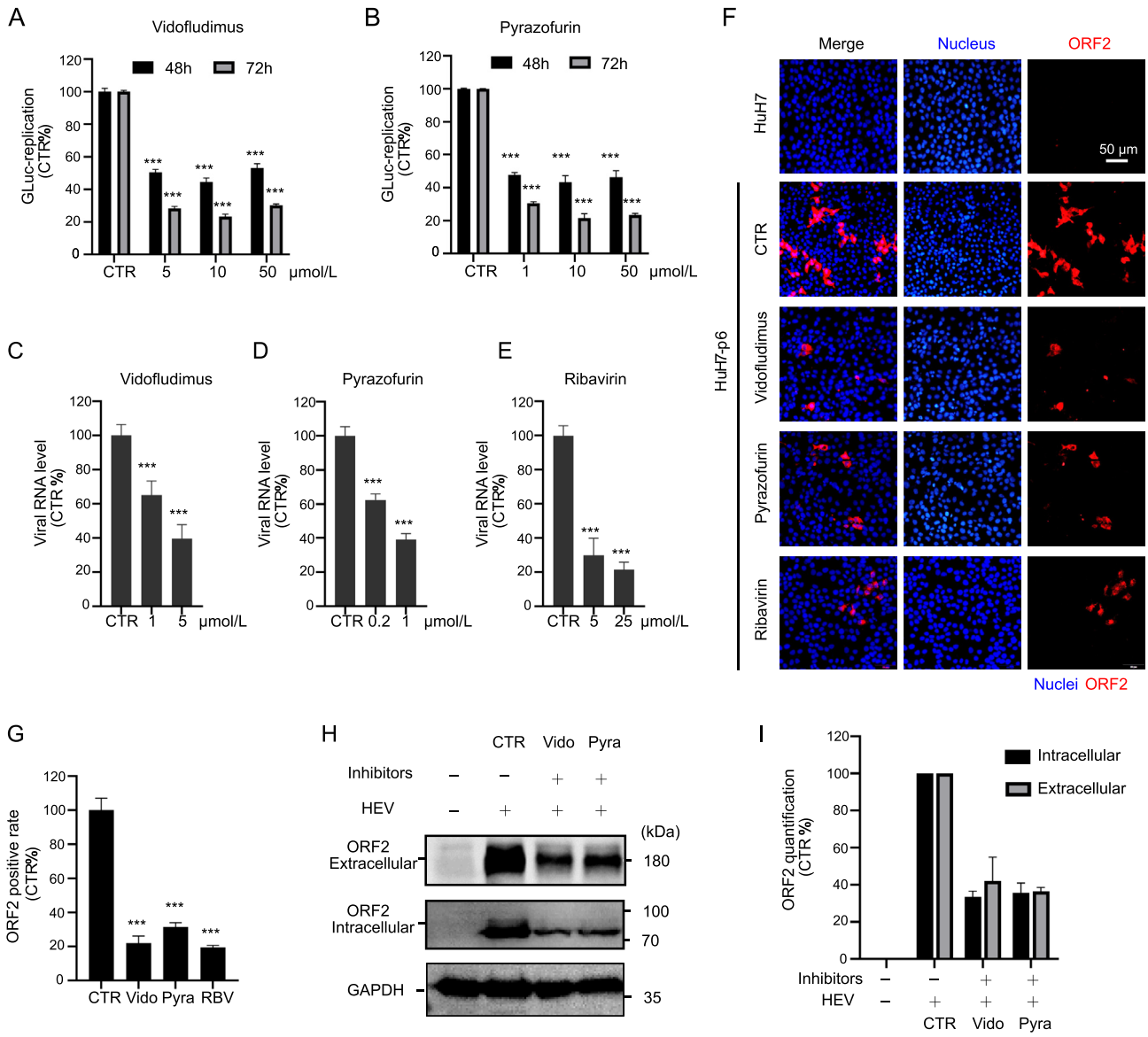

Fig. 2. Vidofludimus calcium and pyrazofurin exert potent antiviral effects in both HEV replicon and infectious models. **A-B** The antiviral effect of vidofludimus calcium (**A**) and pyrazofurin (**B**) was measured in Huh7-p6-Gluc cell model at 48 and 72 h post-treatment (n = 3). **C–E** Antiviral activity of vidofludimus calcium (**C**), pyrazofurin (**D**) and ribavirin (**E**) was measured by RT-qPCR in HuH7-p6 infectious model at 72 h post-treatment (n = 8). **F** Immunofluorescence staining of HEV ORF2 protein (red) in HuH7-p6 infectious model treated with vidofludimus calcium (5 μmol/L), pyrazofurin (1 μmol/L) or ribavirin (25 μmol/L) at 72-h post-treatment. Hoechst (blue) was applied to visualize nuclei. (Scale bar, 50 μm). **G** Quantification of HEV-positive cells by immunofluorescence staining in HEV-p6 cells after 72 h of drug treatment with vidofludimus calcium (5 μmol/L), pyrazofurin (1 μmol/L) or ribavirin (25 μmol/L) (n = 5–8). **H** Western blot analysis of intracellular and extracellular viral ORF2 protein in Huh7-p6 model treated with vidofludimus calcium (5 μmol/L) or pyrazofurin (1 μmol/L) at 72-h post-treatment. **I** Grayscale quantification of intracellular and extracellular ORF2 proteins in Western blot assay by ImageJ (version 1.53k) (n = 3). CTR, untreated control; Vido, vidofludimus calcium; Pyra, pyrazofurin; RBV, ribavirin. Data were normalized to the untreated control (CTR) (set as 100%). Data are presented as means ± SEM (Standard error of the mean). (*, $P < 0.05$; **, $P < 0.01$; ***, $P < 0.001$.)

1 (IC_{50} < 0.02 μmol/L), followed by donor 3 (IC_{50}: 0.29 μmol/L) and donor 4 (IC_{50}: 0.22 μmol/L), but less efficient in donor 2 (60.28 μmol/L) (Fig. 4B, and Supplementary Fig. S4E–H). The quantification of viral RNA by RT-qPCR (Fig. 4C) and immunofluorescence staining of ORF2 protein (Fig. 4D) further confirmed the anti-HEV potency of both drugs without toxicity on organoids (Supplementary Fig. S5). In sum, vidofludimus

Table 1
Summary of the clinical development status of vidofludimus calcium and pyrazofurin and their therapeutic windows against HEV.

Name	Development pipeline	Condition	CC50 (μmol/L)	IC50 against HEV (μmol/L)	SI index
Vidofludiumus calcium	Phase 3	• Relapsing-remitting multiple sclerosis • SARS-CoV-2 infection	160	2.54	63
Pyrazofurin	Phase 2	• Ovarian cancer • Colorectal carcinoma	391	0.16	2444

Note: CC_{50} represents the half-maximum cytotoxic concentration, IC_{50} represents the half-maximal inhibitory concentration, and SI Index represents selectivity index: $SI = CC_{50}/IC_{50}$.

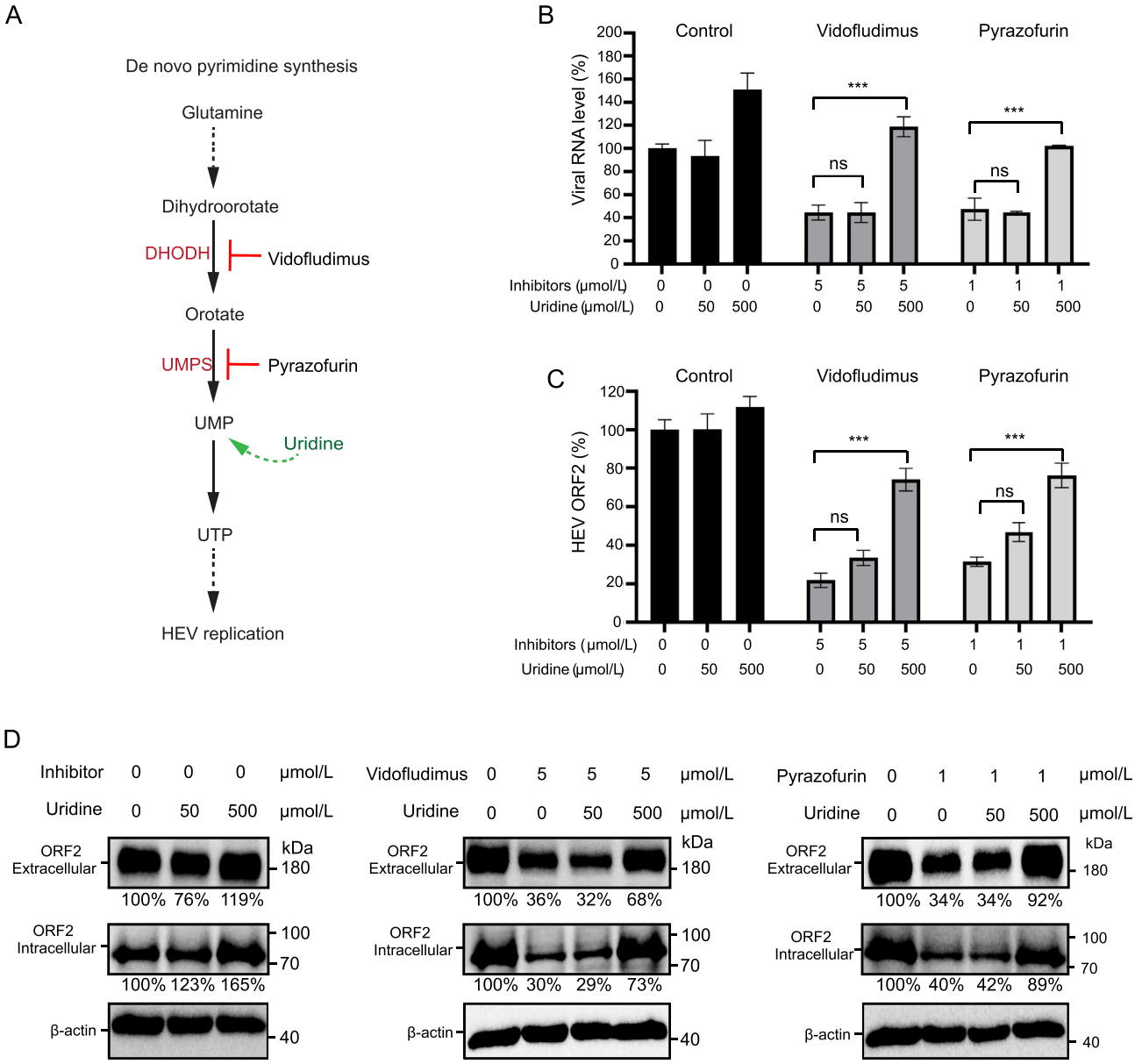

Fig. 3. Supplementation of exogenous uridine reversed the anti-HEV effect of vidofludimus calcium and pyrazofurin. **A** Schematic illustration of *de novo* pyrimidine biosynthesis. DHODH, dihydroorotate dehydrogenase; UMPS, uridine monophosphate synthetase; UMP, uridine monophosphate; UTP, uridine-5′-triphosphate. **B** HEV RNA in HuH7 cell based HEV-p6 model was quantified by RT-qPCR after 72 h of drug treatment with or without the supplement of exogenous uridine (n = 8). **C** Quantification of HEV-positive cells by immunofluorescence staining in HuH7 cell based HEV-p6 cells after 72 h of drug treatment with or without the supplement of exogenous uridine (n = 10). **D** Western blot analysis of intracellular and extracellular viral ORF2 protein in HuH7 cell based HEV-p6 model treated after 72 h of drug treatment with or without the supplement of exogenous uridine. Grayscale quantification of intracellular and extracellular ORF2 proteins in Western blot assay was performed by ImageJ (version 1.53k). Data were normalized to the untreated control (set as 100%). Data are presented as means ± SEM. (*, $P < 0.05$; **, $P < 0.01$; ***, $P < 0.001$.)

calcium and pyrazofurin exhibited anti-HEV activity in primary human organoids derived from different individuals.

3.4. *Ribavirin treatment failure-associated HEV mutants are highly sensitive to vidofludimus calcium or pyrazofurin treatment*

Mutations (Y1320H or G1634R) in the RNA-dependent RNA polymerase (RdRp) of genotype 3 HEV have been reportedly associated with ribavirin treatment failure in chronic hepatitis E patients (Debing et al., 2014, 2016). Given the clinical relevance, we generated two single mutants (M1: Y1320H and M2: G1634R) and a double mutant (M1+2: G1634R/Y1320H) based on the HEV-3 infectious clone Kernow-C1 p6 (GenBank accession no. JQ679013) (Supplementary Fig. S6A). Immunofluorescence staining confirmed the robust replication of all these mutants (Supplementary Fig. S6B). The number of HEV-positive cells was quantified (Supplementary Fig. S6C). Consistent with previous studies (Debing et al., 2014, 2016; Wang et al., 2023), two single mutants exhibit significantly higher ratios of HEV-positive cells compared with wild type (WT). In contrast, the double mutant strain does not exhibit enhanced levels of HEV, probably due to the incompatibility of these two mutations. The IC_{50} values of ribavirin in M1 (17.59 μmol/L) and M2 (14.17 μmol/L) was higher compared with that of wild-type HEV strain (IC_{50} = 8.26 μmol/L) (Supplementary Figs. S6D and E).

Next, we profiled the antiviral activity of vidofludimus calcium and pyrazofurin against different HEV mutants. Excitingly, two drugs were highly efficient against all HEV mutants. We observed potent and dose-

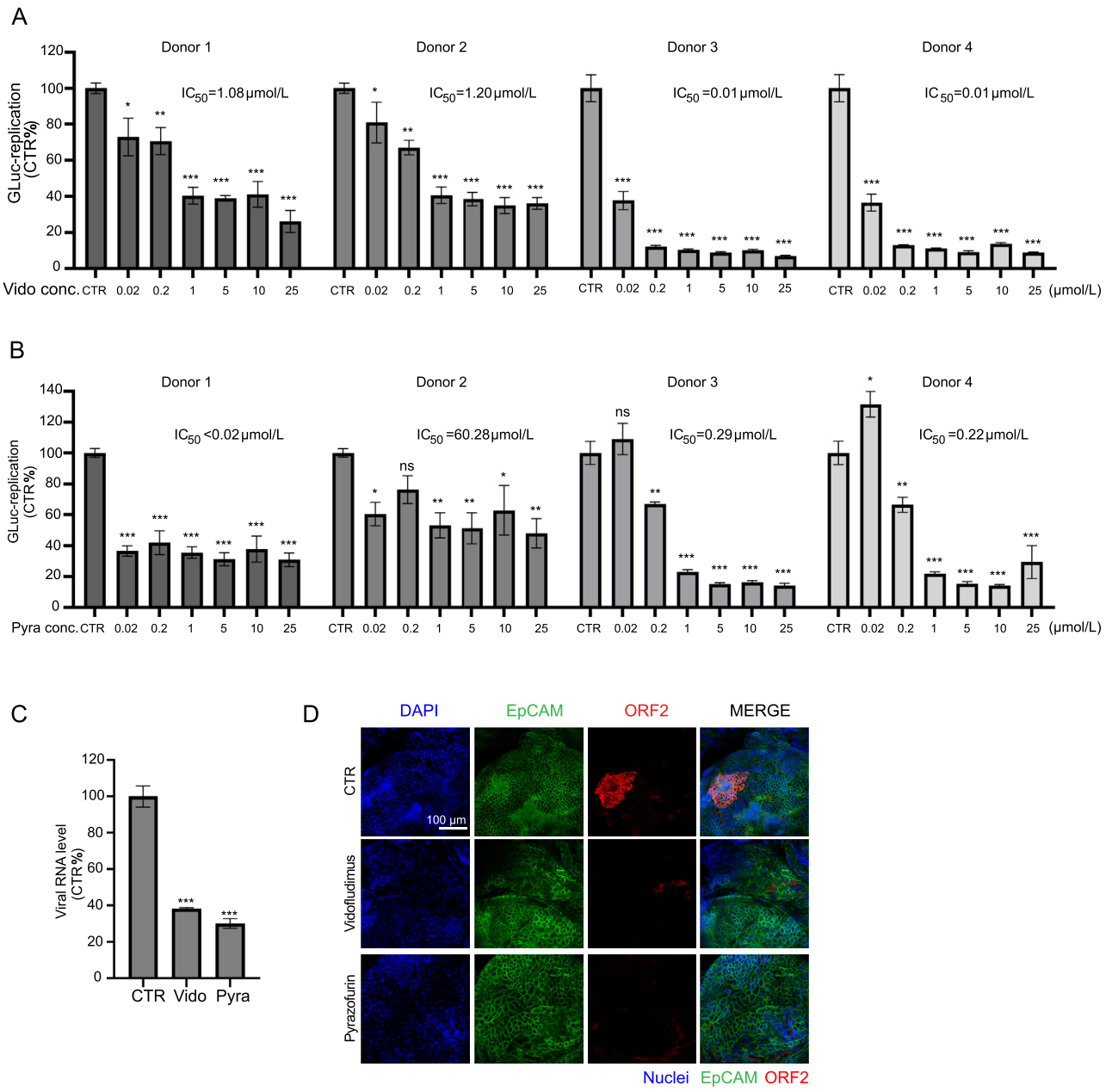

Fig. 4. Vidofludimus calcium and pyrazofurin robustly inhibit HEV replication in human primary liver organoids models. **A** The anti-HEV effect of vidofludimus calcium was measured after 3 days of drug treatment in p6-Gluc model based on the organoids derived from four different donors (n = 6–8). **B** The anti-HEV effect of pyrazofurin was measured after 3 days of drug treatment in p6-Gluc model based on the organoids derived from four different donors (n = 6–8). The 50% inhibitory concentration (IC_{50}) values were calculated using GraphPad Prism. **C** The inhibitory effect of vidofludimus calcium (25 μmol/L) and pyrazofurin (25 μmol/L) was measured by RT-qPCR in human primary liver organoids (donor 1) based HEV p6 infectious model (n = 4). **D** Immunofluorescence staining of viral ORF2 protein (red) in organoids based HEV p6 infectious model after 72 h of treatment with vidofludimus calcium (25 μmol/L) or pyrazofurin (25 μmol/L). DAPI (blue) and EpCAM (green) were applied to visualize nuclei and epithelial cellular adhesion molecule, respectively. (Scale bar, 100 μm). CTR, untreated control. Data were normalized to the untreated control (set as 100%). Data are presented as means ± SEM. (*, $P < 0.05$; **, $P < 0.01$; ***, $P < 0.001$.)

dependent inhibition of HEV based on HEV-positive cell quantification, but no cell toxicity (Fig. 5 and Supplementary Fig. S7). The dose-response curves indicated that HEV mutants, as compared to WT, are comparably sensitive to the treatments (Fig. 5). For instance, the calculated IC_{50} value of vidofludimus calcium is 2.54 μmol/L to WT, 2.33 μmol/L to M1, 1.90 μmol/L to M2, and 2.22 μmol/L to M1+2 (Fig. 5A and B). Notably, the peak plasma concentration (C_{max}) of vidofludimus calcium used in relapsing-remitting multiple sclerosis is 8.738–14.571 μmol/L (Muehler et al., 2020a; Fox et al., 2022). And the C_{max} of vidofludimus calcium used to combat SARS-CoV-2 infection in patients hospitalized with COVID-19 is 14.323–14.57 μmol/L (Vehreschild et al., 2022). That means the IC_{50} values of vidofludimus calcium against WT and mutant HEV strains are 4.6–7.6-fold lower than its plasma concentrations under the current regimens. These convincing results indicate that vidofludimus calcium and pyrazofurin are not only broadly against WT and mutant HEV strains, but also possess great potential for clinical application in hepatitis E treatment.

3.5. *Vidofludimus calcium and pyrazofurin synergizes IFN-α against HEV*

In real-world implementation, the combination of multiple antiviral drugs is a common strategy to enhance antiviral efficacy, limit toxicity,

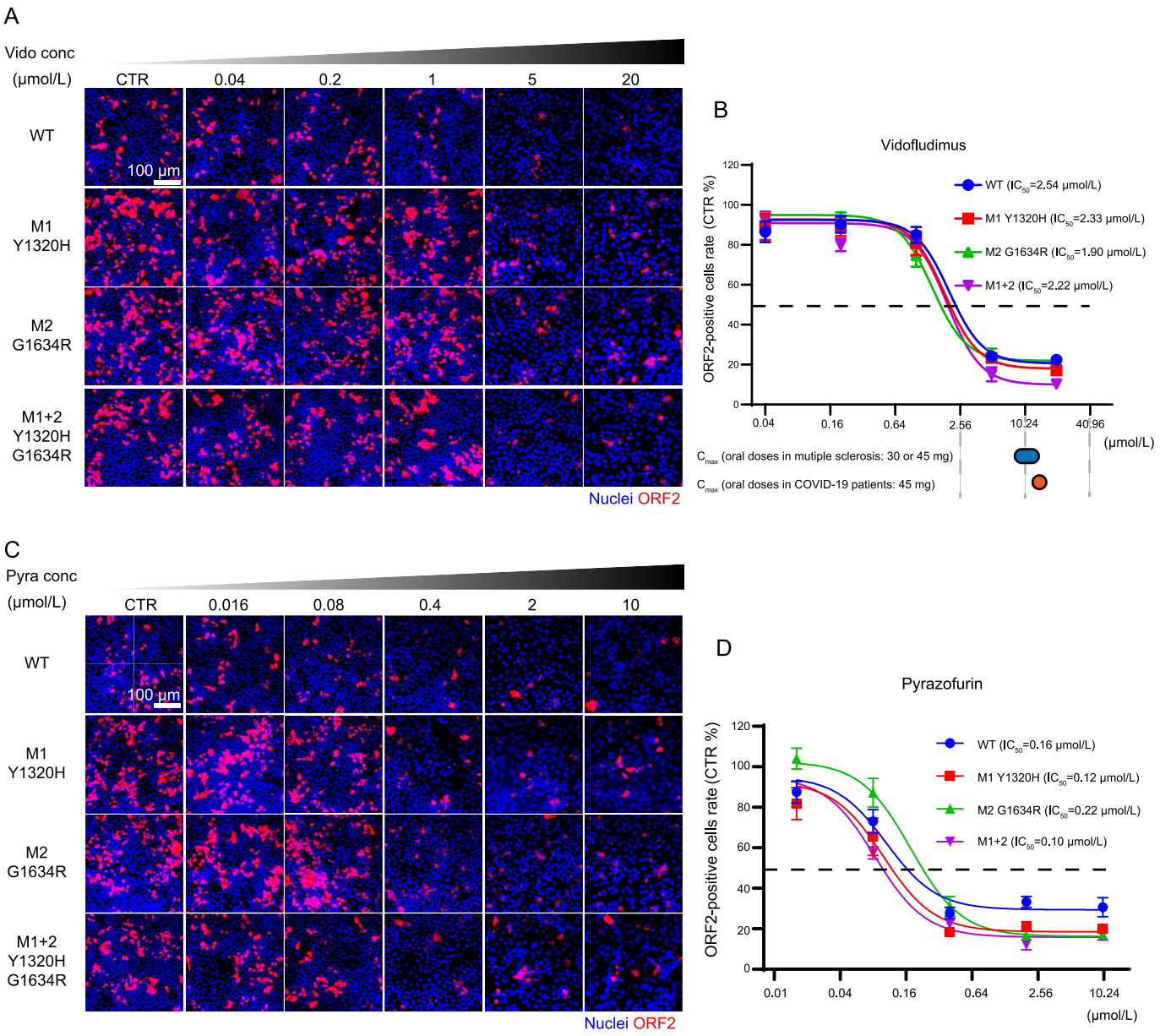

Fig. 5. Determination of IC_{50} values of vidofludimus calcium and pyrazofurin in WT and ribavirin treatment failure-associated HEV mutants. **A, C** Immunofluorescence staining of viral ORF2 protein (red) in WT and HEV mutants after 72 h treatment with vidofludimus calcium (**A**) and pyrazofurin (**C**). **B, D** The IC_{50} values of vidofludimus calcium (**B**) and pyrazofurin (**D**) against WT and mutant HEV strains were calculated using GraphPad Prism software based on the quantification of immunofluorescence staining. CTR, untreated control. Data were normalized to the untreated control (set as 100%). Data are presented as means ± SEM.

and avoid drug resistance. This strategy contributes to the rapid reduction of viral load, the constraint of virus transmission, and improved patient outcomes. Therefore, we evaluated the combinatory effects of these two drugs with IFN-α or ribavirin, the off-label antivirals for chronic hepatitis E (Fig. 6 and Supplementary Fig. S8). The combination with IFN-α exerted an apparent synergistic effect for both drugs, particularly at concentrations ranging from 0.2 to 20 μmol/L vidofludimus calcium with 100–1000 IU IFN-α and 0.1–1 μmol/L pyrazofurin with 100–1000 IU IFN-α. In contrast, their combination with ribavirin did not exhibit an apparent synergistic effect.

4. Discussion

Drug repurposing has gained substantial traction due to its compelling advantages. Successful examples that bring medications with known safety profiles to new patient populations also exist in the field of viral hepatitis. For instance, the HIV reverse transcriptase inhibitors (e.g., tenofovir disoproxil fumarate) are repurposed to treat HBV infection (Kitrinos et al., 2014). The farnesyltransferase inhibitor lonafarnib for treating progeria and progeroid laminopathies has been granted breakthrough therapy for treating hepatitis D virus infection (Dhillon, 2021). It is estimated that the number of repurposed drugs entering the regulatory-approval pipeline is rising and could account for about 20%–30% of all drugs approved every year (Cha et al., 2018). Thus, to meet the urgent needs for treating HEV infection, more efforts are demanded to repurpose drug candidates, a strategy that can find breakthrough therapy options.

In this study, our drug repurposing screen identifies two novel anti-HEV entities. Vidofludimus calcium is the next-generation DHODH inhibitor, and pyrazofurin selectively inhibits UMPS. They exert their anti-HEV effect through the depletion of pyrimidine nucleotide pool. The inhibition of pyrimidine synthesis by targeting DHODH or UMPS shows promise for the treatment of auto-immune diseases or viral infections (Wang et al., 2016; Chen et al., 2019; Muehler et al., 2020b).

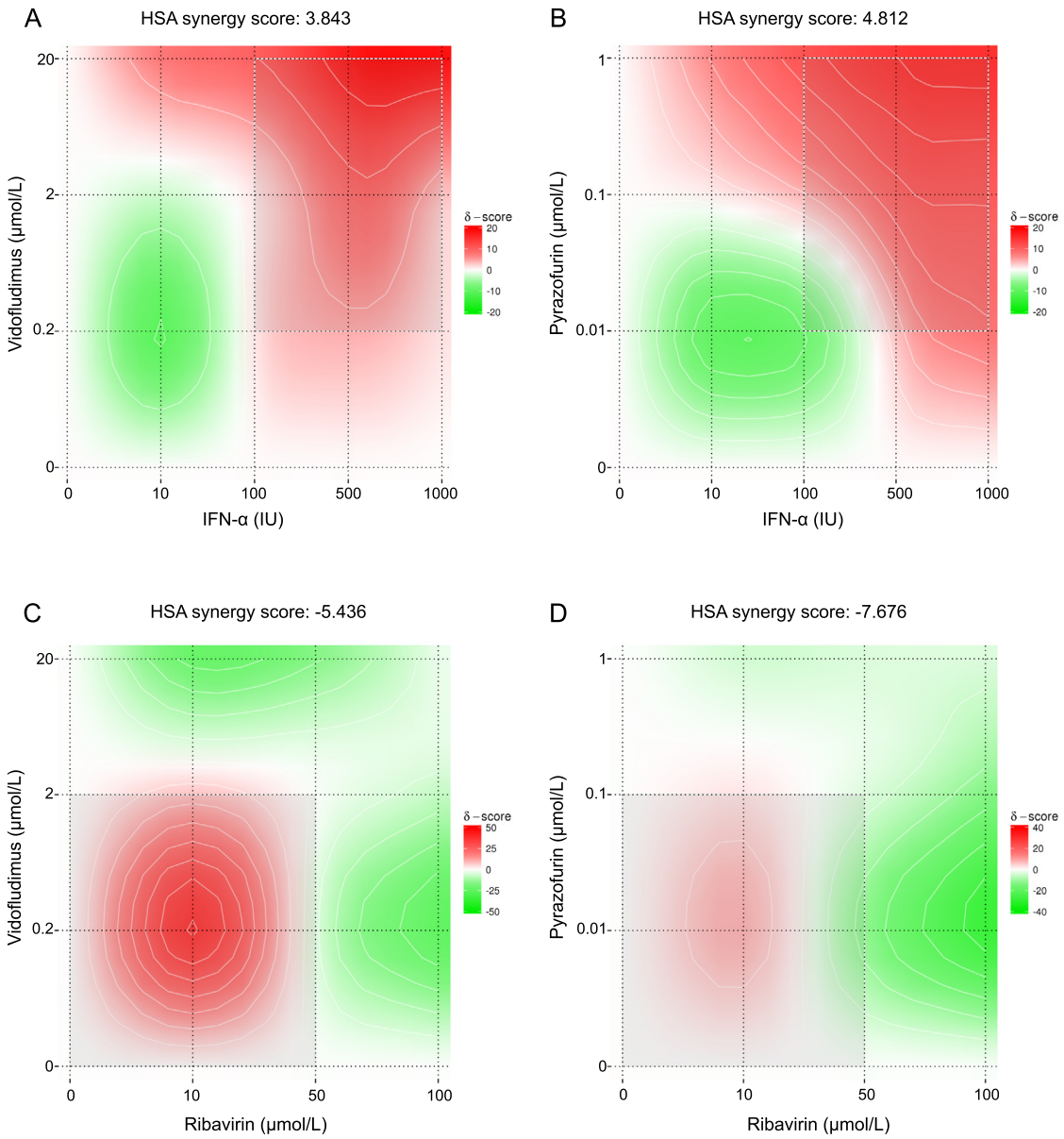

Fig. 6. Determination of the synergistic effect in combination with IFN-α or ribavirin. **A-B** Synergy distribution of pairwise combination of IFN-α and vidofludimus calcium (**A**) or pyrazofurin (**B**) (n = 4). **C-D** Synergy distribution of pairwise combination of ribavirin and vidofludimus calcium (**C**) or pyrazofurin (**D**) (n = 4). The synergy score was calculated by SynergyFinder 3.0 (https://synergyfinder.fimm.fi/). HSA, highest single agent.

Currently, there are two U.S. FDA-approved DHODH inhibitors on the market. Leflunomide is used for the management of rheumatoid arthritis, and its active analog teriflunomide is used for the treatment of relapsing-remitting multiple sclerosis. However, safety concerns have arisen due to post-marketing reports of severe liver injury from patients receiving these two drugs (Aithal, 2011). This has resulted in the FDA issuing black-box warnings for hepatic injury for both drugs in 2010 and 2012 (FDA, 2010, 2012). Thus, they are not applicable for being repurposed as anti-HEV drugs, since HEV already causes pathogenic damage in liver.

In contrast, vidofludimus calcium is the new generation DHODH inhibitor with high selectivity and specificity. They are structurally distinct from leflunomide and teriflunomide and exhibit favorable safety profiles (Jones et al., 2021). Vidofludimus calcium has been well-studied in over 1400 healthy volunteers or patients with immune-related conditions with a safety and tolerability profile similar to placebo (Muehler et al., 2020a; Fox et al., 2022). Vidofludimus calcium has advanced in phase 3 clinical development for patients with multiple sclerosis (Therapeutics) or hospitalized with COVID-19 (ClinicalTrials.gov NCT04379271). It showed clinical antiviral activity while preserving SARS-CoV-2 humoral response in patients (Vehreschild et al., 2022). Encouragingly, we observed a large therapeutic window between these two drugs' CC_{50} and IC_{50} values against HEV (Table 1). For vidofludimus calcium, its IC_{50} values against HEV are even 4.6–7.6-fold lower than the achievable therapeutic doses in patients (Fig. 5). Based on the antiviral efficacy, and the favorable safety profile identified in earlier clinical studies, our study calls the initiation of clinical studies to evaluate the effect of these two drugs for treating chronic hepatitis E.

The resilience of antiviral drugs against fast-evolving RNA viruses presents a significant challenge in identifying new therapeutic approaches for timely disease control. HEV encodes only one non-structural multifunctional and multidomain protein (ORF1), which serves as a good candidate for anti-HEV drugging strategies. In this context, efforts have been made to identify potent candidates that target different functional subdomains of ORF1. For instance, zinc salts were reported to directly inhibit the activity of viral RNA-dependent RNA

polymerase (RdRp), leading to inhibition of viral replication (Kaushik et al., 2017). Based on in silico screening methods, compounds that potentially inhibit the function of methyltransferase or helicase of ORF1 were also discovered (Hooda et al., 2022; Pedroni et al., 2022). These compounds may hold potential as direct acting antivirals in controlling HEV infection. In addition, host metabolic pathways are exquisite reservoirs of energy and building blocks to viruses and are essential for successful replication and pathogenesis of viruses. DHODH and UMPS, the cognate targets of these two drugs identified in this study, are key factors essential for host nucleotide metabolism. Encouragingly, both drugs are highly efficient and comparable against WT as well as ribavirin treatment failure-associated mutants (Fig. 5). Thus, targeting host factors to cease viral infection, offers distinct advantages in terms of increased threshold to viral resistance (Dwek et al., 2022).

Antiviral monotherapies are often found to be suboptimal in clinical settings with respect to efficacy. Instead, combination regimens can enhance antiviral potency, reduce the emergence of drug-resistant variants, and lower the dose of each component in the combination (Wagoner et al., 2022). Concurrently combination of drugs with distinct mode-of-action offers opportunities to discover synergistic drug combinations. In this study, the combination with IFN-α exerted an apparent synergistic effect for both drugs (Fig. 6). IFN-α exerts its antiviral effect solely relying on the induction of antiviral interferon-stimulated genes (ISGs) via the JAK-STAT pathway. Interestingly, we and others previously found that the inhibition of the pyrimidine pathway concurrently triggered ISG induction, independent of the classical JAK-STAT pathway (Wang et al., 2016; Luthra et al., 2018). Whether these two distinct ISG induction actions correlate with the synergistic effects we observed merits further investigation. Nevertheless, the results provide a proof-of-concept for treating HEV infection with the combination of conventional and novel regimens.

5. Conclusion

In sum, vidofludimus calcium and pyrazofurin, with their mechanisms of action centered on depleting the pyrimidine nucleotide pool, have demonstrated potent anti-HEV activity in both *in vitro* and *ex vivo* models. Our findings provide compelling evidence for the clinical evaluation of vidofludimus calcium and pyrazofurin as potential treatments for chronic hepatitis E, offering hope for improved patient outcomes and disease control.

Data availability

All data generated or analyzed during this study are included in this published article.

Ethics statement

The isolation and culture of organoids were conducted using liver tissues obtained during liver transplantation at the Erasmus Medical Center Rotterdam. The utilization of liver tissues for research was approved by the Medical Ethical Council of the Erasmus MC, with informed consent obtained from donors (MEC-2014-060).

Author contributions

Hongbo Guo: conceptualization, funding acquisition, resources, supervision, writing-review and editing. Dan Liu and Kuan Liu: investigation, methodology, visualization, data curation and formal analysis. Yao Hou, Chunyang Li, Qiudi Li, Xiaohui Ding, Monique M A Verstegen, Jikai Zhang, Lingli Wang and Yibo Ding: investigation, visualization, data curation and validation. Renxian Tang, Xiucheng Pan, Kuiyang Zhen and Luc J W van der Laan: writing reviewing, resources. Qiuwei Pan: resources, supervision, writing-review. Wenshi Wang: conceptualization, funding acquisition, resources, supervision, writing-review and editing.

Conflict of interest

The authors declared that they do not have anything to disclose regarding funding or conflict of interest with respect to this manuscript.

Acknowledgments

This work was funded by the National Natural Science Foundation of China (32270161, 32100117, 32100118), the Natural Science Foundation of Jiangsu Province of China (BK20210899, BK20210900, BK20210901), Research Grant of Jiangsu Commission of Health, China (ZD2021036), and the Starting Grant for Talents of Xuzhou Medical University (D2021007, D2021008).

Appendix A. Supplementary data

Supplementary data to this article can be found online at https://doi.org/10.1016/j.virs.2023.11.006.

References

Aithal, G.P., 2011. Hepatotoxicity related to antirheumatic drugs. Nat. Rev. Rheumatol. 7, 139–150.
Cha, Y., Erez, T., Reynolds, I.J., Kumar, D., Ross, J., Koytiger, G., Kusko, R., Zeskind, B., Risso, S., Kagan, E., Papapetropoulos, S., Grossman, I., Laifenfeld, D., 2018. Drug repurposing from the perspective of pharmaceutical companies. Br. J. Pharmacol. 175, 168–180.
Chen, S., Ding, S., Yin, Y., Xu, L., Li, P., Peppelenbosch, M.P., Pan, Q., Wang, W., 2019. Suppression of pyrimidine biosynthesis by targeting DHODH enzyme robustly inhibits rotavirus replication. Antivir. Res. 167, 35–44.
Debing, Y., Gisa, A., Dallmeier, K., Pischke, S., Bremer, B., Manns, M., Wedemeyer, H., Suneetha, P.V., Neyts, J., 2014. A mutation in the hepatitis E virus RNA polymerase promotes its replication and associates with ribavirin treatment failure in organ transplant recipients. Gastroenterology 147, 1008–1011 e1007; quiz e1015-1006.
Debing, Y., Ramiere, C., Dallmeier, K., Piorkowski, G., Trabaud, M.A., Lebosse, F., Scholtes, C., Roche, M., Legras-Lachuer, C., De Lamballerie, X., Andre, P., Neyts, J., 2016. Hepatitis E virus mutations associated with ribavirin treatment failure result in altered viral fitness and ribavirin sensitivity. J. Hepatol. 65, 499–508.
Del Bello, A., Guilbeau-Frugier, C., Josse, A.G., Rostaing, L., Izopet, J., Kamar, N., 2015. Successful treatment of hepatitis E virus-associated cryoglobulinemic membranoproliferative glomerulonephritis with ribavirin. Transpl. Infect. Dis. 17, 279–283.
Desai, A.N., Mohareb, A.M., Elkarsany, M.M., Desalegn, H., Madoff, L.C., Lassmann, B., 2022. Viral hepatitis E outbreaks in refugees and internally displaced populations, sub-Saharan Africa, 2010-2020. Emerg. Infect. Dis. 28, 1074–1076.
Dhillon, S., 2021. Lonafarnib: first approval. Drugs 81, 283–289.
Dwek, R.A., Bell, J.I., Feldmann, M., Zitzmann, N., 2022. Host-targeting oral antiviral drugs to prevent pandemics. Lancet 399, 1381–1382.
Fox, R.J., Wiendl, H., Wolf, C., De Stefano, N., Sellner, J., Gryb, V., Rejdak, K., Bozhinov, P.S., Tomakh, N., Skrypchenko, I., Muehler, A.R., 2022. A double-blind, randomized, placebo-controlled phase 2 trial evaluating the selective dihydroorotate dehydrogenase inhibitor vidofludimus calcium in relapsing-remitting multiple sclerosis. Ann Clin Transl Neurol 9, 977–987.
Guinault, D., Ribes, D., Delas, A., Milongo, D., Abravanel, F., Puissant-Lubrano, B., Izopet, J., Kamar, N., 2016. Hepatitis E virus-Induced cryoglobulinemic glomerulonephritis in a nonimmunocompromised person. Am. J. Kidney Dis. 67, 660–663.
Hooda, P., Chaudhary, M., Parvez, M.K., Sinha, N., Sehgal, D., 2022. Inhibition of hepatitis E virus replication by novel inhibitor targeting methyltransferase. Viruses 14, 1778.
Ianevski, A., Giri, A.K., Aittokallio, T., 2022. SynergyFinder 3.0: an interactive analysis and consensus interpretation of multi-drug synergies across multiple samples. Nucleic Acids Res. 50, W739–W743.
Jones, S.W., Penman, S.L., French, N.S., Park, B.K., Chadwick, A.E., 2021. Investigating dihydroorotate dehydrogenase inhibitor mediated mitochondrial dysfunction in hepatic in vitro models. Toxicol. Vitro 72, 105096.
Kamar, N., Abravanel, F., Lhomme, S., Rostaing, L., Izopet, J., 2015. Hepatitis E virus: chronic infection, extra-hepatic manifestations, and treatment. Clin Res Hepatol Gastroenterol 39, 20–27.
Kamar, N., Del Bello, A., Abravanel, F., Pan, Q., Izopet, J., 2022. Unmet needs for the treatment of chronic hepatitis E virus infection in Immunocompromised patients. Viruses 14, 2116.
Kamar, N., Izopet, J., Tripon, S., Bismuth, M., Hillaire, S., Dumortier, J., Radenne, S., Coilly, A., Garrigue, V., D'alteroche, L., Buchler, M., Couzi, L., Lebray, P., Dharancy, S., Minello, A., Hourmant, M., Roque-Afonso, A.M., Abravanel, F., Pol, S., Rostaing, L., Mallet, V., 2014. Ribavirin for chronic hepatitis E virus infection in transplant recipients. N. Engl. J. Med. 370, 1111–1120.
Kamar, N., Marion, O., Abravanel, F., Izopet, J., Dalton, H.R., 2016. Extrahepatic manifestations of hepatitis E virus. Liver Int. 36, 467–472.

Karki, P., Malik, S., Mallick, B., Sharma, V., Rana, S.S., 2016. Massive hemolysis causing renal failure in acute hepatitis E infection. J Clin Transl Hepatol 4, 345–347.
Kaushik, N., Subramani, C., Anang, S., Muthumohan, R., Shalimar, Nayak, B., Ranjith-Kumar, C.T., Surjit, M., 2017. Zinc salts block hepatitis E virus replication by inhibiting the activity of viral RNA-dependent RNA polymerase. J. Virol. 91, e00754-17.
Kinast, V., Burkard, T.L., Todt, D., Steinmann, E., 2019. Hepatitis E Virus Drug Development. Viruses 11, 485.
Kitrinos, K.M., Corsa, A., Liu, Y., Flaherty, J., Snow-Lampart, A., Marcellin, P., Borroto-Esoda, K., Miller, M.D., 2014. No detectable resistance to tenofovir disoproxil fumarate after 6 years of therapy in patients with chronic hepatitis B. Hepatology 59, 434–442.
Li, P., Liu, J., Li, Y., Su, J., Ma, Z., Bramer, W.M., Cao, W., De Man, R.A., Peppelenbosch, M.P., Pan, Q., 2020. The global epidemiology of hepatitis E virus infection: a systematic review and meta-analysis. Liver Int. 40, 1516–1528.
Li, P., Li, Y., Wang, Y., Liu, J., Lavrijsen, M., Li, Y., Zhang, R., Verstegen, M.M.A., Wang, Y., Li, T.C., Ma, Z., Kainov, D.E., Bruno, M.J., De Man, R.A., Van Der Laan, L.J.W., Peppelenbosch, M.P., Pan, Q., 2022. Recapitulating hepatitis E virus-host interactions and facilitating antiviral drug discovery in human liver-derived organoids. Sci. Adv. 8, eabj5908.
Luthra, P., Naidoo, J., Pietzsch, C.A., De, S., Khadka, S., Anantpadma, M., Williams, C.G., Edwards, M.R., Davey, R.A., Bukreyev, A., Ready, J.M., Basler, C.F., 2018. Inhibiting pyrimidine biosynthesis impairs Ebola virus replication through depletion of nucleoside pools and activation of innate immune responses. Antivir. Res. 158, 288–302.
Mcbride, J.T., 1985. Ribavirin and RSV: a new approach to an old disease. Pediatr. Pulmonol. 1, 294–295.
Muehler, A., Kohlhof, H., Groeppel, M., Vitt, D., 2020a. Safety, tolerability and pharmacokinetics of vidofludimus calcium (IMU-838) after single and multiple Ascending oral doses in healthy male Subjects. Eur. J. Drug Metab. Pharmacokinet. 45, 557–573.
Muehler, A., Peelen, E., Kohlhof, H., Groppel, M., Vitt, D., 2020b. Vidofludimus calcium, a next generation DHODH inhibitor for the Treatment of relapsing-remitting multiple sclerosis. Mult Scler Relat Disord 43, 102129.
Netzler, N.E., Enosi Tuipulotu, D., Vasudevan, S.G., Mackenzie, J.M., White, P.A., 2019. Antiviral candidates for treating hepatitis e virus infection. Antimicrob Agents Chemother 63, e00003–19.
Pedroni, L., Dellafiora, L., Varra, M.O., Galaverna, G., Ghidini, S., 2022. In silico study on the Hepatitis E virus RNA Helicase and its inhibition by silvestrol, rocaglamide and other flavagline compounds. Sci. Rep. 12, 15512.
Pischke, S., Hartl, J., Pas, S.D., Lohse, A.W., Jacobs, B.C., Van Der Eijk, A.A., 2017. Hepatitis E virus: infection beyond the liver? J. Hepatol. 66, 1082–1095.
Qu, C., Xu, L., Yin, Y., Peppelenbosch, M.P., Pan, Q., Wang, W., 2017. Nucleoside analogue 2'-C-methylcytidine inhibits hepatitis E virus replication but antagonizes ribavirin. Arch. Virol. 162, 2989–2996.
Roessler, H.I., Knoers, N., Van Haelst, M.M., Van Haaften, G., 2021. Drug repurposing for rare diseases. Trends Pharmacol. Sci. 42, 255–267.
Shukla, P., Nguyen, H.T., Faulk, K., Mather, K., Torian, U., Engle, R.E., Emerson, S.U., 2012. Adaptation of a genotype 3 hepatitis E virus to efficient growth in cell culture depends on an inserted human gene segment acquired by recombination. J. Virol. 86, 5697–5707.
Therapeutics, P.-I.. https://imux.com/pipeline/.
FDA, 2010. FDA Drug Safety Communication: New boxed warning for severe liver injury with arthritis drug Arava (leflunomide). https://www.fda.gov/drugs/postmarket-drug-safety-information-patients-and-providers/fda-drug-safety-communication-new-boxed-warning-severe-liver-injury-arthritis-drug-arava-leflunomide (Accessed date: 1 August 2023).
FDA, 2012. FDA Approved Labeling Text. www.fda.gov/drugs. https://www.accessdata.fda.gov/drugsatfda_docs/label/2012/202992s000lbl.pdfVehreschild (Accessed date: 1 August 2023).
Vehreschild, M., Atanasov, P., Yurko, K., Oancea, C., Popov, G., Smesnoi, V., Placinta, G., Kohlhof, H., Vitt, D., Peelen, E., Mihajlovic, J., Muehler, A.R., 2022. Safety and efficacy of vidofludimus calcium in patients hospitalized with COVID-19: a double-blind, randomized, placebo-controlled, phase 2 trial. Infect. Dis. Ther. 11, 2159–2176.
Velavan, T.P., Pallerla, S.R., Johne, R., Todt, D., Steinmann, E., Schemmerer, M., Wenzel, J.J., Hofmann, J., Shih, J.W.K., Wedemeyer, H., Bock, C.T., 2021. Hepatitis E: an update on One Health and clinical medicine. Liver Int. 41, 1462–1473.
Wagoner, J., Herring, S., Hsiang, T.Y., Ianevski, A., Biering, S.B., Xu, S., Hoffmann, M., Pohlmann, S., Gale Jr., M., Aittokallio, T., Schiffer, J.T., White, J.M., Polyak, S.J., 2022. Combinations of host- and virus-targeting antiviral drugs confer synergistic suppression of SARS-CoV-2. Microbiol. Spectr. 10, e0333122.
Wang, Y., Wang, W., Xu, L., Zhou, X., Shokrollahi, E., Felczak, K., Van Der Laan, L.J., Pankiewicz, K.W., Sprengers, D., Raat, N.J., Metselaar, H.J., Peppelenbosch, M.P., Pan, Q., 2016. Cross Talk between nucleotide synthesis pathways with cellular Immunity in constraining hepatitis E virus replication. Antimicrob. Agents Chemother. 60, 2834–2848.
Wang, W., Cui, J., Ma, H., Lu, W., Huang, J., 2021. Targeting pyrimidine metabolism in the era of precision cancer medicine. Front. Oncol. 11, 684961.
Wang, B., Mahsoub, H.M., Li, W., Heffron, C.L., Tian, D., Hassebroek, A.M., Leroith, T., Meng, X.J., 2023. Ribavirin treatment failure-associated mutation, Y1320H, in the RNA-dependent RNA polymerase of genotype 3 hepatitis E virus (HEV) enhances virus replication in a rabbit HEV infection model. mBio 14, e0337222.
Webb, G.W., Dalton, H.R., 2019. Hepatitis E: an underestimated emerging threat. Ther Adv Infect Dis 6, 2049936119837162.
Xiong, R., Zhang, L., Li, S., Sun, Y., Ding, M., Wang, Y., Zhao, Y., Wu, Y., Shang, W., Jiang, X., Shan, J., Shen, Z., Tong, Y., Xu, L., Chen, Y., Liu, Y., Zou, G., Lavillette, D., Zhao, Z., Wang, R., Zhu, L., Xiao, G., Lan, K., Li, H., Xu, K., 2020. Novel and potent inhibitors targeting DHODH are broad-spectrum antivirals against RNA viruses including newly-emerged coronavirus SARS-CoV-2. Protein Cell 11, 723–739.